

# Determination of the critical threshold for the occurrence of fires in the Parque Nacional de Brasília (Brazil) through temporal analysis using spectral indices

Lucas Inácio da Silva<sup>1</sup> 

Gustavo Macedo de Mello Baptista<sup>2</sup> 

## Keywords

Analysis  
Biome  
Google Earth Engine  
Fire  
Monitoring

## Abstract

The Brazilian Savannah is one of the largest biomes in Brazil. Unfortunately, human pressure is aggravating the degradation processes of the biome and, together with the drought processes, fire events are a major concern. Monitoring tools must be designed, especially those involving the concepts of remote sensing, in anticipation of the fire phenomenon, mitigating the devastating effects. Therefore, the present research aims to determine the critical threshold for the occurrence of fires through the diagnosis of the conditions of greenness, humidity and senescence of the vegetation using the temporal analysis of Sentinel-2 images in the Parque Nacional de Brasília. Therefore, it is necessary to quantitatively determine each condition through the analysis of past events, determining the criticality threshold that conditions the region to present conditions that favor the onset of a fire, as well as the construction of an algorithm, in the Google Earth Engine. The study area is the Parque Nacional de Brasília, with the image data collection Harmonized Sentinel-2 MSI: MultiSpectral Instrument, Level-1C inside the Google Earth Engine. The algorithm aims to build a masking system to remove materials from the scenes, as well as the calculation of the NDVI, NDII, PSRI and dNBR indices, extracting the data through the mask of burned pixels. It was possible to identify six periods of fire occurrence, the data extraction allowed the statistical determination of the threshold, which was 0,580 for the NDVI, 0,015 for the NDII and 0,150 for the PSRI.

<sup>1</sup> Universidade Católica de Brasília - UCB, Brasília, DF, Brazil. [silva.lucasinacio.11@gmail.com](mailto:silva.lucasinacio.11@gmail.com)

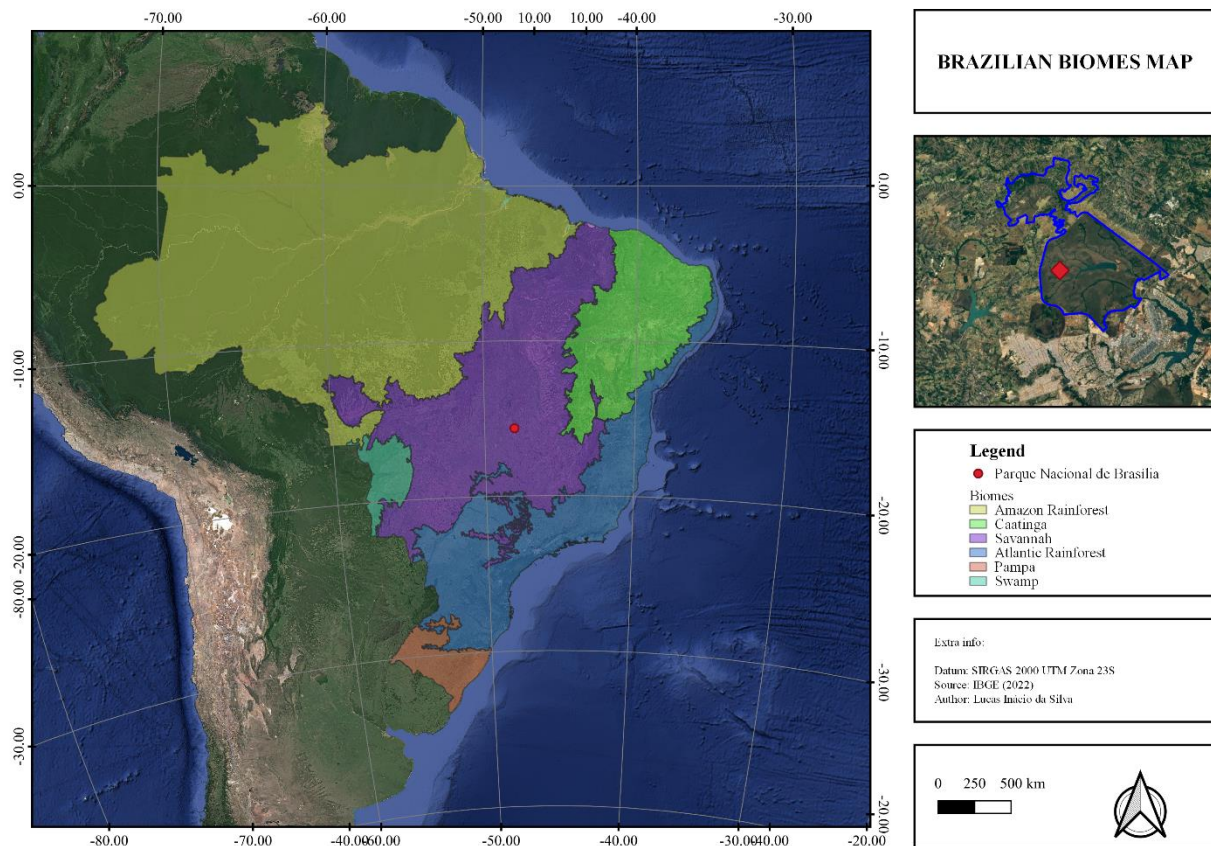
<sup>2</sup> Universidade de Brasília - UnB, Brasília, DF, Brazil. [gmbaptista@gmail.com](mailto:gmbaptista@gmail.com)

## INTRODUCTION

The Savannah Biome is considered one of the largest existing biomes in the Brazilian

territory, with an approximate extension of 2 million square kilometers and is located in the central region of the Brazilian territory, as seen in Figure 1, being a natural border of the Amazon Rainforest and Caatinga biomes (COLLI et al., 2020).

Figure 1 – Map of Brazilian Biomes



Source: The authors (2022).

The biome has a rich biodiversity and an extensive list of fauna and flora species, however, it suffers from increasing human pressure, marked by the expansion of agricultural activities and forest fires, which can occur both naturally or by human action (HOFMANN et al., 2021).

The Cerrado has dry seasons, which provide an environment conducive to the occurrence of fire events, raising questions about the fundamental role of prevention, surveillance, detection and firefighting tools (HOFMANN et al., 2021; VERNOOIJ et al., 2021). Such events also function as maintenance of ecosystems, but management and monitoring are essential in order to keep the impacts under control, avoiding the spread of flames and the danger to biodiversity (RIBEIRO et al., 2019).

Fire monitoring techniques and systems should be designed to take precedence over the event, providing support for decision-making, so

a good monitoring system aims to help manage efforts, producing specific intervention solutions in such events (BARMPOUTIS et al., 2020).

Considering that territorial monitoring systems usually involve large dimensions, remote sensing emerges as a powerful science and tool, allowing the creation of mechanisms with great potential for data mass analysis. (BARMPOUTIS et al., 2020).

Fire events demonstrate the environmental fragility of ecosystems, in particular those of native vegetation, and studying the severity of these events is important for verifying the ecological, economic and physical consequences of the affected region, strategically coordinating mitigation actions (FASSNACHT et al., 2021; FERNÁNDEZ-MANSO; QUINTANO, 2020).

Baptista et al. (2018) and Bento-Gonçalves et al. (2019) suggest that the evaluation, through remote sensing, of the indicators of greenness, humidity and senescence can be an important

milestone to determine the methodologies for monitoring areas that may have fuel potential, since these areas have different pixels from the areas that did not burn, indicating fire susceptibility.

The occurrence of fires, whether of anthropic causes or not, represent a potential danger to fauna, flora and human lives, as can be seen in events in Portugal, during the year 2017 (BAPTISTA *et al.*, 2018) or in several countries such as Australia, Brazil, Canada, the D.R. Congo, Greece, Indonesia, Russia, Spain and the USA (BENTO-GONÇALVES, 2022). The adoption of tools and policies for the prevention and prediction of fires in a solid and efficient way becomes necessary for the correct targeting of intervention measures in order to minimize the impact generated by the spread of a fire.

Management strategies are usually done in a timely manner and the adoption of the use of spatial data can expand actions related to integrated fire management, so it is possible to raise the hypothesis that it is possible to evaluate the fire events that occurred in the National Park from Brasília, starting in 2015 (the year in which Sentinel-2 images began) and stipulating critical limits of greenness, humidity and senescence in these areas.

Therefore, the present work has as its general objective the determination of the critical threshold for the occurrence of fires

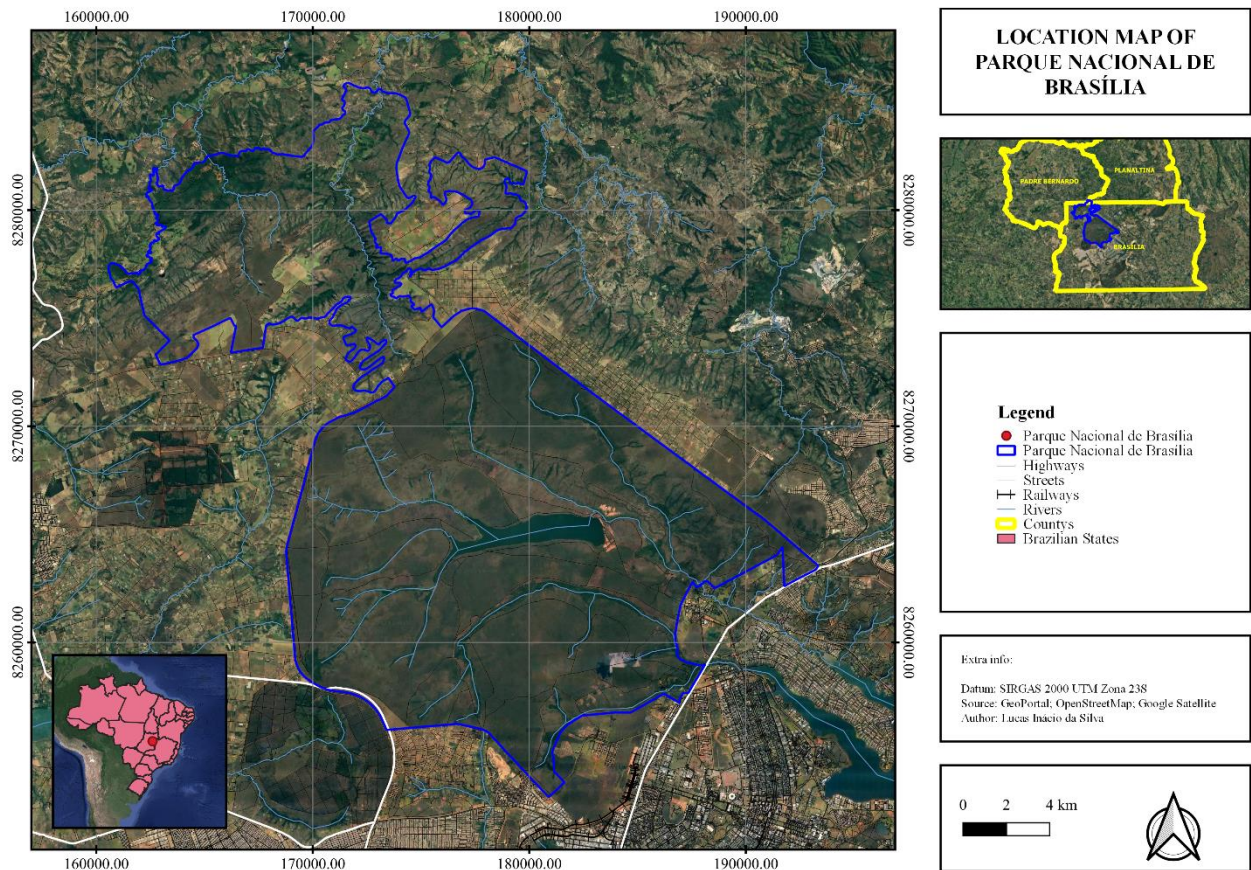
through the diagnosis of the conditions of greenness, humidity and senescence of the vegetation using the temporal analysis of Sentinel-2 images in the Parque Nacional de Brasília. Therefore, it is necessary to quantitatively determine each condition through the analysis of past events, determining the threshold of criticality that conditions the region to be a potential ignitor for fire events, as well as the construction of an algorithm, in Google Earth Engine – GEE, based on the proposed methodology.

## METHODS

### *Study area*

The study area in question is the Parque Nacional de Brasília, located in the northwest of the Distrito Federal. The park is a Unidade de Conservação de Proteção Integral, which is a law created territory to protect the circumscribed region, and was created on November 29, 1961, under Decree No. 241 and has approximately 42,389 hectares, encompassing the administrative regions of Plano Piloto, Sobradinho, and Brazlândia, as well as a portion of the municipalities people from Padre Bernardo and Planaltina, as seen in Figure 2.

Figure 2 – Location of Parque Nacional de Brasília

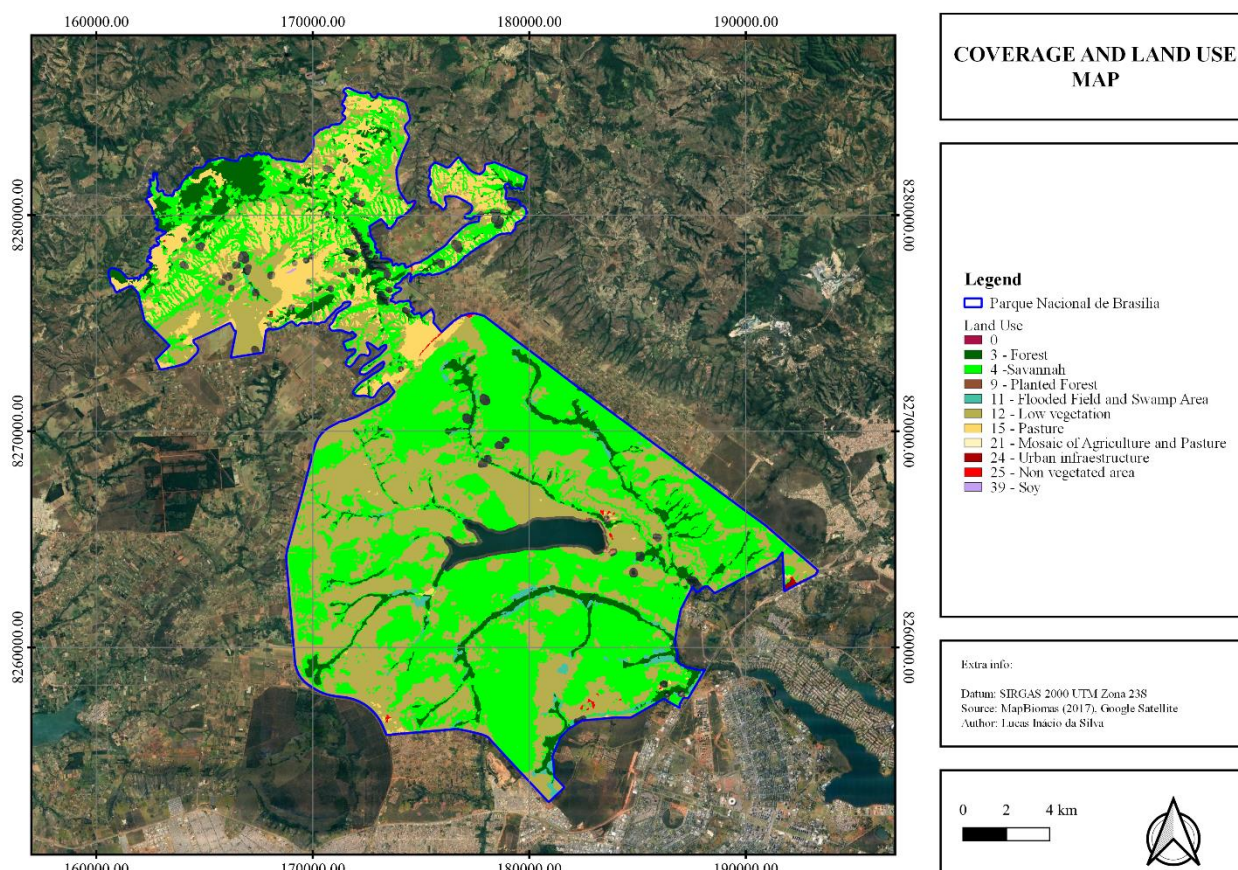


Source: The authors (2022).

The cover and use of the soil, as it is an integrally protected Conservation Unit, is predominantly made up of forest, savannah and

grassland plant formations, as observed in the Figure 3.

Figure 3 – Coverage and Land Use of Parque Nacional de Brasília



Source: The authors (2022).

### GIS

The GEE will be used, which is an online platform for processing, viewing and manipulating geographic data (GORELICK *et al.*, 2017). Due to its great processing capacity, it will be possible to develop a script capable of performing the necessary analyzes for the periods under study, which mitigates the large data manipulation time required in conventional means of processing in remote sensing.

### Data Collection

It was used the collection of multispectral images from the Copernicus program called Harmonized Sentinel-2 MSI: MultiSpectral Instrument, Level-1C was used. The images of this segment, according to the European Space Agency, have already been systematically processed by ground control stations, which in this case is the “Payload Data Ground Segment”.

This collection slides the pixel values of images taken after January 25, 2022, to respect the range of old data values.

The products of this collection are already sent from the Payload Data Ground Segment with the analyzed telemetry, decompressed, with the necessary corrections and radiometric and geometric calibrations and with resampled values for reflectance data. The product does not have a solution for atmospheric calibration, which will be performed by applying the Sensor Invariant Atmospheric Correction, present in a library in the GEE, developed and validated by MarcYin (2019a) and MarcYin (2019b), being used by Nursaputra *et al.* (2021) and Carella *et al.* (2022).

The normal products Level-1C and Level-2A were not used because, for the former, the values of the old images are not in the same ranges as the new images, which could harm automatic processes within the platform, and for the second, there are no corrected images for the entire period you want to search.

### Research methodological procedures

The procedures used to obtain the results and objective of the research will be described in this section.

### Determining event periods

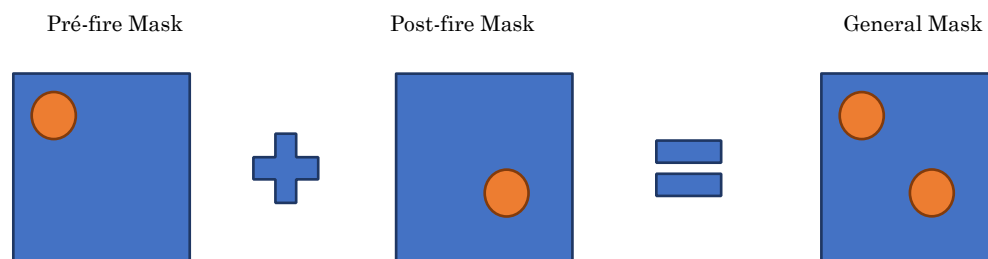
For the development of the methodology, it was necessary to identify periods in which fire events occurred within the Parque Nacional de Brasília. Therefore, with the help of the Instituto Nacional de Pesquisas Espaciais (which is a research unit of the Brazilian Ministry of Science, Technology and Innovations) systems, six periods of occurrence of events were identified, which, for each event,

it was necessary to identify two images, one pre- and one post-fire.

### Spatial Filtering of scenes

Aiming to improve the automatic processes built within the platform, mitigating the negative effects arising from the use of spectral indices, spatial masks were used to filter the elements in question, allowing only the regions with plant material to be analyzed. For this, it used spectral indices to identify clouds, cloud shadows, water and finally, as a way to guarantee that the analyzed regions do not suffer from non-vegetable interference. Figure 4 shows how the general mask was obtained.

Figure 4 – Methodology for creating the general event mask



Source: The authors (2022).

To identify the clouds, the Sentinel Cloud Probability product was used, provided by the Sentinel Hub, developed on the “Sentinel2-Cloud-Detector” algorithm, together with the “LightGBM” library. The value of 50% was used, which indicates that the pixels that were 50% sure that the content adjacent to the pixel was really a cloud were filtered.

For the identification of cloud shadows, the concepts obtained in Magno et al. (2021), the “Cloud Shadow Index” – CSI, systematized in Equation 1, and filtered at the thresholds of interest for identifying shadows, thanks to the specific behavior of the “Shortwave Infrared” band of the “Multispectral Instrument” sensor

$$CSI = \frac{(1 - \rho_{2,2})^2}{2 \times 2_{2,2}} \quad \text{Equation 1}$$

The Normalized Difference Water Index – NDWI, proposed by McFeeters (1996) and the Sentinel Water Mask, proposed by Milczarek et al. (2017). The indices, as they can be obtained, respectively, by Equation 2 e Equation 3, emphasize water bodies.

$$NDWI = \frac{\rho_{0.55} - \rho_{0.65}}{\rho_{0.55} + \rho_{0.65}} \quad \text{Equation 2}$$

$$SWM = \frac{\rho_{0.45} - \rho_{0.55}}{\rho_{0.85} + \rho_{1.60}} \quad \text{Equation 3}$$

The pre- and post-fire masks were obtained by calculating the aforementioned indices for the images in question. After calculating both, the overall mask of the event was calculated for each period, consisting of pre and post-fire masks. It served to ensure that the analysis within the platform worked for any period in question, considering that pixels not present in an image and that were not in another would not be analyzed, thus guaranteeing the homogeneity of the analysis.

Still aiming at the platform procedures, it was decided to create a buffer of 120 meters (or 12 pixels of the sensor) to mitigate the material transition effects.

### Spectral Indices

In this section, the central methodology of the research will be demonstrated.

### Normalized Difference Vegetation Index (NDVI)

The “Normalized Difference Vegetation Index” – NDVI shows the greenness of vegetation based on the absorption of red and near infrared through simple math of the band between the red (0.65  $\mu\text{m}$ ) and near-infrared (0.85  $\mu\text{m}$ )

layers) which intends to create representativeness between the targets of greater emission of red and infrared (ROUSE et al., 1974). To calculate the NDVI, we used the Equation 4.

$$NDVI = \frac{\rho_{0.85} - \rho_{0.65}}{\rho_{0.85} + \rho_{0.65}} \quad \text{Equation 4}$$

The index varies from -1 to 1, where values below 0.2 show the absence of photosynthetic activity, that is, the index shows the degree of greenness of the vegetation through the gain of the red band over the near infrared band, highlighting the vegetation with greener aspect (DUAN et al., 2017), and values in the range from 0.2 to 1 represent, gradually, the level of greenness of vegetation according to its health standards (SILVA; BAPTISTA, 2015).

### *Normalized Difference Infrared Index (NDII)*

The “Normalized Difference Infrared Index” – NDII explains the humidity of the tree canopy by means of band mathematics similar to the NDVI, however, in this case, the NIR information layers are used together with the SWIR of 1.60  $\mu\text{m}$  (HARDISKY31 et al., 1983). To calculate the NDII, Equation 5 was used.

$$NDII = \frac{\rho_{0.85} - \rho_{1.60}}{\rho_{0.85} + \rho_{1.60}} \quad \text{Equation 5}$$

The index ranges from -1 to 1, whose values below 0 indicate that the NIR reflectance is greater than the SWIR reflectance, which may indicate water stress in the vegetation (SRIWONGSITANON et al., 2016, SRIWONGSITANON et al., 2015).

### *Plant Senescence Reflectance Index (PSRI)*

The Plant Senescence Reflectance Index – PSRI measures the senescence and health of the vegetation through the dynamics of pigmentation influenced by the chemistry of the plant which produces different spectral responses (MERZLYAK et al., 1999).

The index demonstrates the sensitivity of chlorophyll in relation to carotenoids, and negative values represent the green plant mesh with high chlorophyll composition, the range from -0.1 to 0.2 indicates the beginning of the aging stage and the final intervals indicate the final stage of canopy senescence, therefore, is a contrary analysis of the numerical scale, when compared to the other indices. Equation 6 demonstrates the calculation of the PSRI.

$$PSRI = \frac{\rho_{0.65} - \rho_{0.45}}{\rho_{0.75}} \quad \text{Equation 6}$$

### *Normalized Burn Ratio (NBR)*

The Normalized Burn Ratio – NBR highlights the burned areas (KEY; BENSON, 1999; KEY, BENSON, 2006), through band mathematics similar to the previous indices and can also serve as a basis for another calculation that is “Differenced Normalized Burn Ratio” – dNBR for the pre- and post-fire periods, more accurately assessing the severity of the event (ROY et al., 2006). The Equation 7 e Equation 8 demonstrate how the data referring to the traverses of the fire events were obtained.

$$NBR = \frac{\rho_{0.85} - \rho_{2.20}}{\rho_{0.85} + \rho_{2.20}} \quad \text{Equation 7}$$

$$dNBR = NBR_{Pré-fogo} - NBR_{Pós-fogo} \quad \text{Equation 8}$$

Table 1 demonstrates the intervals considered by Miller and Thode (2006), considering the Differenced Normalized Burn Ratio by Roy et al. (2006).

**Table 1** – dNBR intervals

Severity level	Range	Color
<b>High Regrowth</b>	-500 a -250	
<b>Low Regrowth</b>	-249 a -100	
<b>Not Burnt</b>	-99 a 100	
<b>Low Severity</b>	101 a 270	
<b>Low Moderate Severity</b>	271 a 440	
<b>Moderate High Severity</b>	441 a 600	
<b>High Severity</b>	661 a 1.300	

Source: Miller and Thode (2006). Adapted by the authors.

The delimitation of the burned regions was based on the regions considered burned, that is, from the value of 101.

### *Determination of the critical threshold*

By means of the burn severity mask, obtained by dNBR, it was possible to segregate the regions of interest for the extraction of pixel values. For each pixel centroid, the values of NDVI, NDII and PSRI were extracted. The PSRI, NDVI, NDII and burn severity values are obtained by calculating the spectral indices of the methodology.

The extracted values were submitted to average statistical calculations for each event. These values served to determine the general

average of the analyzed period, quantitatively determining the value that represents the beginning of the criticality stage for the occurrence of fires.

## **RESULTS AND DISCUSSION**

### *Determining event periods*

Six periods of fire occurrence were determined, which were named Event 1, Event 2, Event 3, Event 4, Event 5 and Event 6. The dates of the images are arranged in Table 2.

**Table 2** – Date of event images

Event	Pre-fire	Post-fire
<b>Event 1</b>	11/08/2017	15/09/2017
<b>Event 2</b>	26/08/2018	10/09/2018
<b>Event 3</b>	13/05/2019	12/07/2019
<b>Event 4</b>	02/04/2020	12/05/2020
<b>Event 5</b>	05/08/2021	09/09/2021
<b>Event 6</b>	02/04/2022	02/05/2022

Source: The authors (2022).

### *Spatial Filtering of scenes*

Filtering through the masks together with the “buffering” process showed a very satisfactory result. It was possible to calculate the overall mask for each event, from the pre and post-fire masks.

The Sentinel Cloud Probability product showed an excellent degree of cloud identification, even using the 50% threshold (recommended for a more homogeneous selection of the product).

The product developed with the expertise of Magno et al. (2021) provides, within the threshold of interest, excellent accuracy in the selection of shaded regions. As found by Magno et al. (2021), the shaded regions could be identified, by recording the spectral behavior of the dry and wet threshold.

The NDWI index showed great efficiency for identifying massive bodies of water, with established thresholds. The literature by Kaplan and Advan (2017) recommends, for

Sentinel-2, the value of 0.1, which was used in the processing.

It was possible to observe, as in Kaplan and Advan (2017), that mountainous regions that produced extensions were mistakenly identified, indicating shaded regions or dark material.

Corroborating with the ideas of Milczarek et al. (2017), with the SWM it was possible to discretize and specialize the water surface with a high degree of precision, also allowing the identification of small bodies of water and rivers with a short border length.

It was observed that the water indices have difficulties to differentiate water bodies

submitted to eutrophication processes, due to the presence of biological material in the structure of the water, as well as the dynamics of the water surface can generate a propensity to specular reflection phenomena, which is the accentuated reflection of the incidence of solar rays, impairing the recognition of the water surface as a water body.

Figure 5 demonstrates how the process identified the materials that should be removed from the scene. It is possible to observe that most of the unwanted material for processing was discretized, and the “buffer” process allowed treating the pixel transition region.

Figure 5 -- Mask demonstration



Source: The authors (2022).

As observed in Santos et al. (2023), the use of masks reduced the confusion and classification of pixels not belonging to the class of vegetation and burned, which were being analyzed in the study. The coverage and use of classification of exposed soil, urban area and water, for example, were well characterized and segregated from the automatic classification for extracting index values.

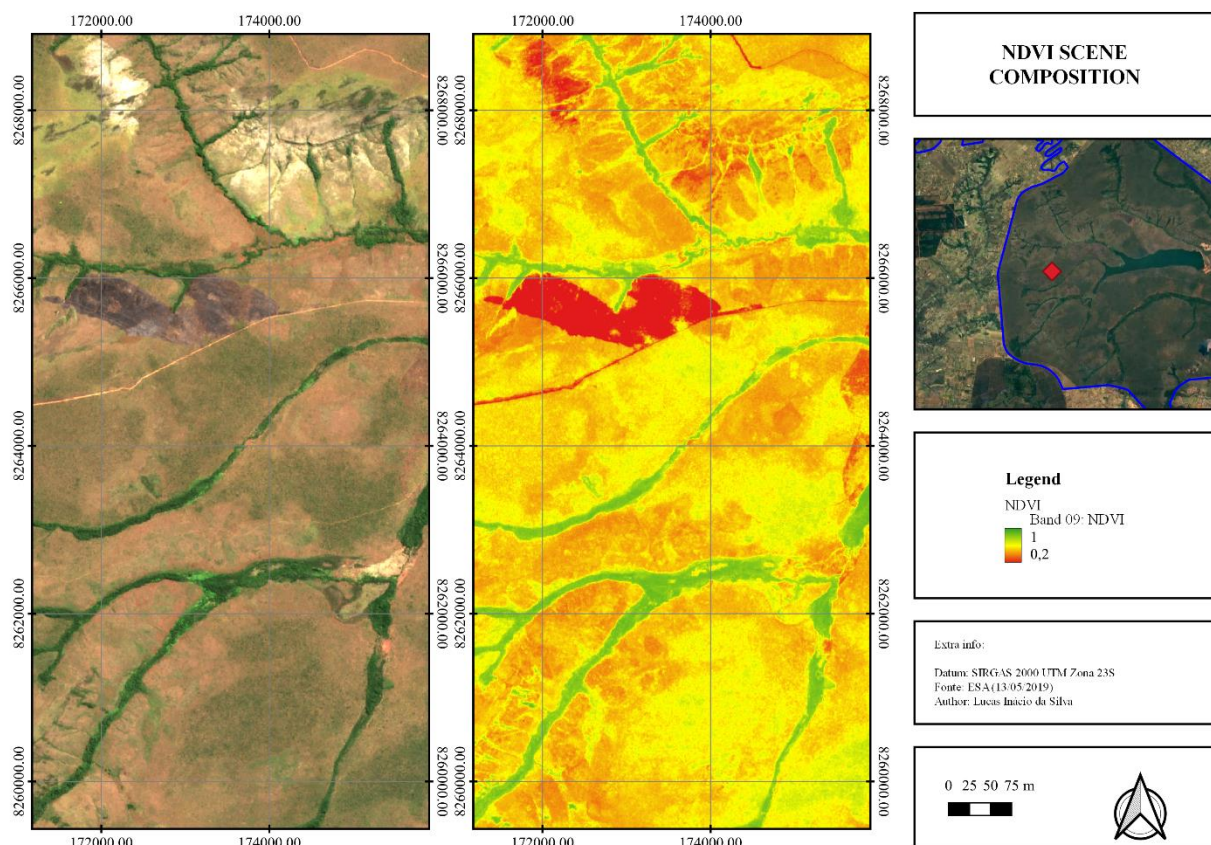
### *Spectral Indices*

The results obtained with the spectral indices explained in the research methodology will be demonstrated.

### *Normalized Difference Vegetation Index (NDVI)*

The NDVI index could be calculated for all the studied periods, and in general, it presented behavior consistent with the research objects. The index presented a problematic behavior in the dry periods, since the absence of rain generated great hydric stress in the vegetation, impairing the photosynthetic activity. Figure 6 shows the index calculation result.

Figure 6 – Example of calculated NDVI



Source: EUROPEAN SPACE AGENCY (n.d.).

Baptista et al. (2018) and Bento-Gonçalves et al. (2019) found mean values of 0.889. This value is considered very high in terms of verdure (considering different climatic and vegetation contexts), and by itself does not affect the region's susceptibility to fire. This research found values close to 0.582. This value already indicates an alert to the degree of stress, since the acceptable threshold for the index is [0.2, 1.0].

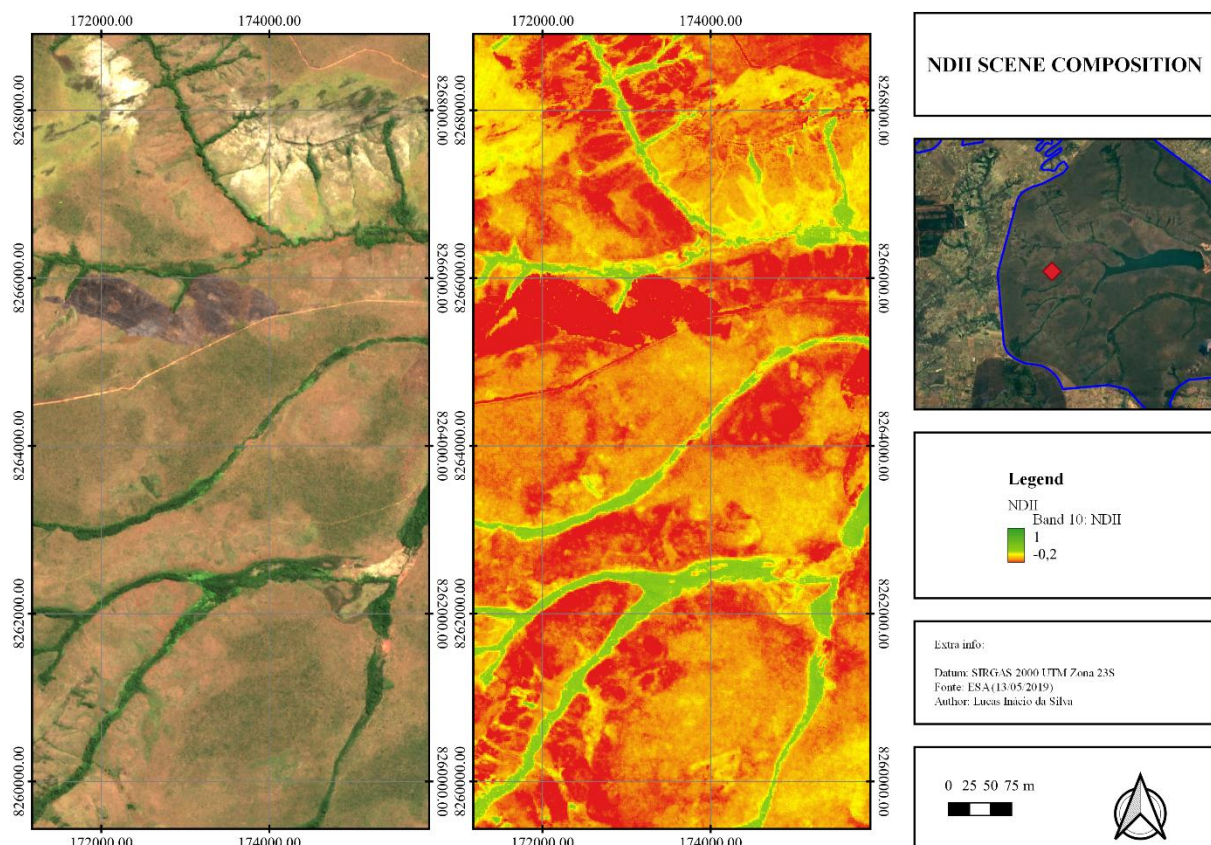
The values found for this index had a high degree of amplitude, indicating a heterogeneous behavior of the vegetation that burned, that is, regions with low and high rates of greenness burned. It is hard to say that the NDVI has a

great impact on determining the fuel potential of vegetation.

### *Normalized Difference Infrared Index (NDII)*

The NDII index could be calculated for all the studied periods, and in general, it presented behavior consistent with the research objects. The index showed great susceptibility to periods of drought, generating a great overestimation of the critical condition of the vegetation, mainly the low and medium size vegetation. Figure 7 shows the index calculation result.

Figure 7 – Example of calculated NDII



Source: EUROPEAN SPACE AGENCY (n.d.).

Baptista et al. (2018) and Bento-Gonçalves et al. (2019) found, for Portugal, mean values of 0.35 and those of the present research found values in the mean of 0.014. The value found indicates that there is an average value close to the vegetation water stress threshold, according to Sriwongsitanon et al. (2015).

According to Baptista et al. (2018), it is expected that the burned regions have lower humidity compared to the unburned areas. The NDII values showed less dispersion than those of the NDVI, indicating that the pixels of the burned regions present a certain degree of similarity among themselves, when the fuel potential is contextualized. It is possible that regions with a high greenness content also burn, but it is expected that regions with a high

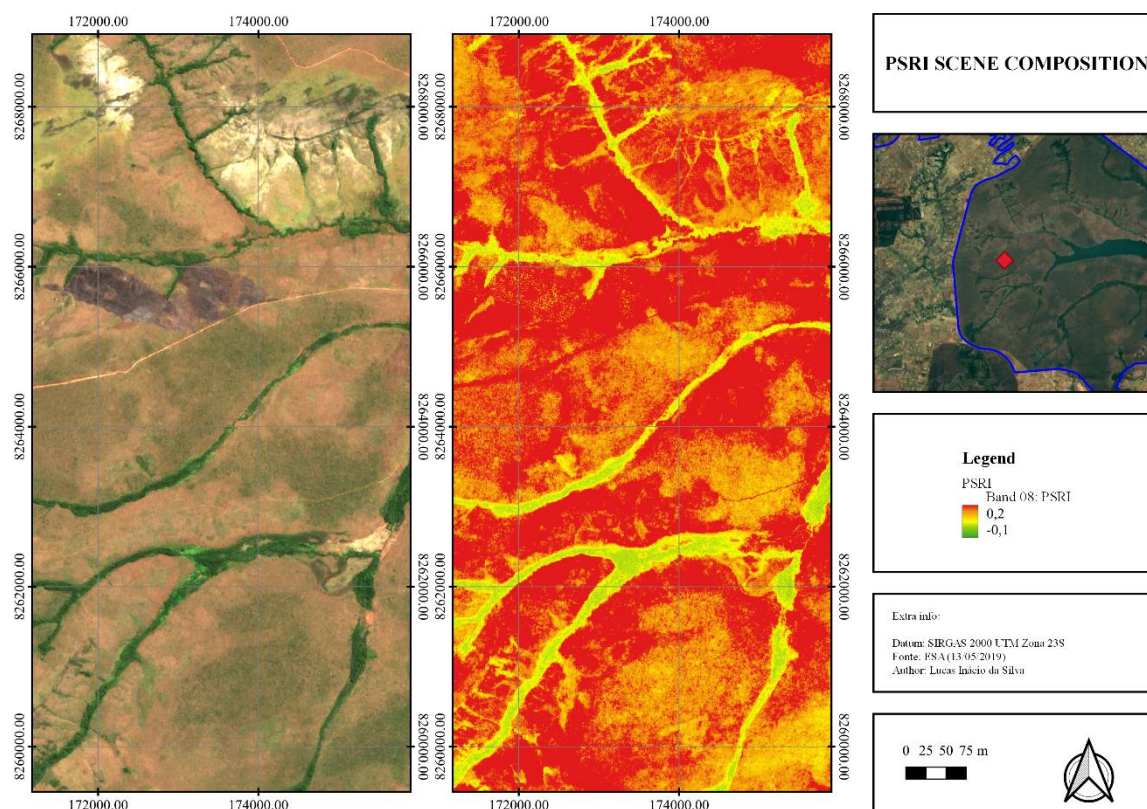
moisture content burn less and are more persistent in the passage of flames.

Also observed by Santos et al. (2023), scars from burns are sometimes confused with water surfaces. The technique used by Santos et al. (2023) involves machine learning, and the one used in the present research involves the combination of water surface identification mask, to remove them from the image to be analyzed.

### *Plant Senescence Reflectance Index (PSRI)*

The PSRI index could be calculated for all periods studied, and in general, it showed behavior consistent with the research objects, as we see the Figure 8.

Figure 8 – Calculated PSRI exaple



Source: EUROPEAN SPACE AGENCE (n.d.).

There was a tendency towards a high average of the values related to the PSRI in the regions that burned, indicating that these regions had a certain degree of senescence. Baptista et al. (2018) and Bento-Gonçalves et al. (2019) found mean values of 0.26 in the burned regions analyzed in their research. This value is within the region considered to be of senescent vegetation.

The values extracted in this study indicated means close to the senescence stage onset interval, which encompasses the interval [0.1, 0.2].

### *Normalized Burn Ratio (NBR)*

The NBR was calculated in the pre and post-fire images, allowing the calculation of the dNBR for each event. The dNBR was used for the automatic creation and extraction of polygons from the burned areas. Within these polygons, pixel values were extracted, necessary for statistical calculations.

Although these are different regions, it was observed by Santos et al. (2023) the NBR was very efficient in identifying regions burned by thermal anomaly, as well as suggesting that this index represents the best proposal for temporal

analyses involving thermal anomalies. It was possible to identify the burned regions with a certain degree of precision, including in the temporal analysis, using the same threshold proposed for the index.

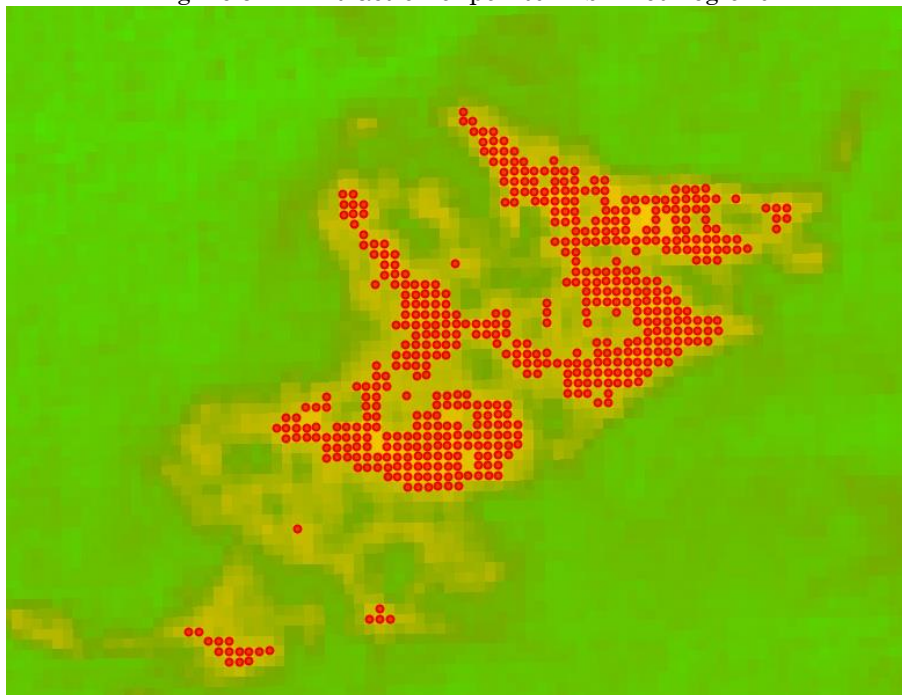
The calculation of dNBR and RdNBR were performed from NBR. It was observed that the dNBR proved to be quite efficient for determining the mask of the burned region, however, when segregated into the severity classes, it showed a certain homogeneous degree of classification of the severity classes, and the RdNBR overestimated such intervals, identifying and mixing the classes of “moderate” and “high severity”, observed in the fires of Geraiis Vieira, Mucugê and Geraiis Machobongo in Santos et al. (2020).

As dNBR showed a better ability to separate the severities, mainly used in homogeneous vegetation, the mask of this index was used, discretizing the burned regions from the unburned ones.

### *Determination of the critical threshold*

The dNBR polygon allowed the extraction of values, as shown in the Figure 9.

Figure 9 - – Extraction of points in burned regions



Source: The authors (2022).

Six tables were extracted from the GEE platform, as exemplified in Table 3. Each table

refers to an analyzed event, so it was possible to perform statistical averages for the 6 events.

**Table 3**– Excerpt from the extracted mass of data

Point	NDII	NDVI	PSRI	Severity
1	0,189	0,714	-0.086	459
2	0.194	0.721	-0.095	471
3	0.180	0,707	-0,081	474
4	0,185	0,716	-0,089	456
5	0,124	0,617	-0,081	460

Source: The authors (2022).

To determine the general critical threshold, we chose to average the values obtained in the 6 events. Systematically demonstrates the values

calculated in the survey, for each year, as well as the suggested final average.

**Table 4** – Systematization of the values obtained

Event	NDVI	NDII	PSRI	Extracted Points
Event 1	0,416	-0,024	0.124	98.095
Event 2	0.504	0.024	0.140	119
Event 3	0,646	0.017	-0,033	68.272
Event 4	0,646	0,023	-0,089	33.968
Event 5	0,670	0,050	0,093	81.928
Event 6	0.612	0.000	0.102	72.950
<b>Critical Threshold</b>	<b>&lt;=0.580</b>	<b>&lt;=0.015</b>	<b>&gt;=0.150</b>	-

Source: The authors (2022).

The aforementioned values show a high degree of coherence, as in the studies by Baptista et al. (2018) and Bento-Gonçalves et al. (2019) and the averages, for the burned regions, of 0.26 for the PSRI, 0.85 for the NDVI and 0.35 for the NDII.

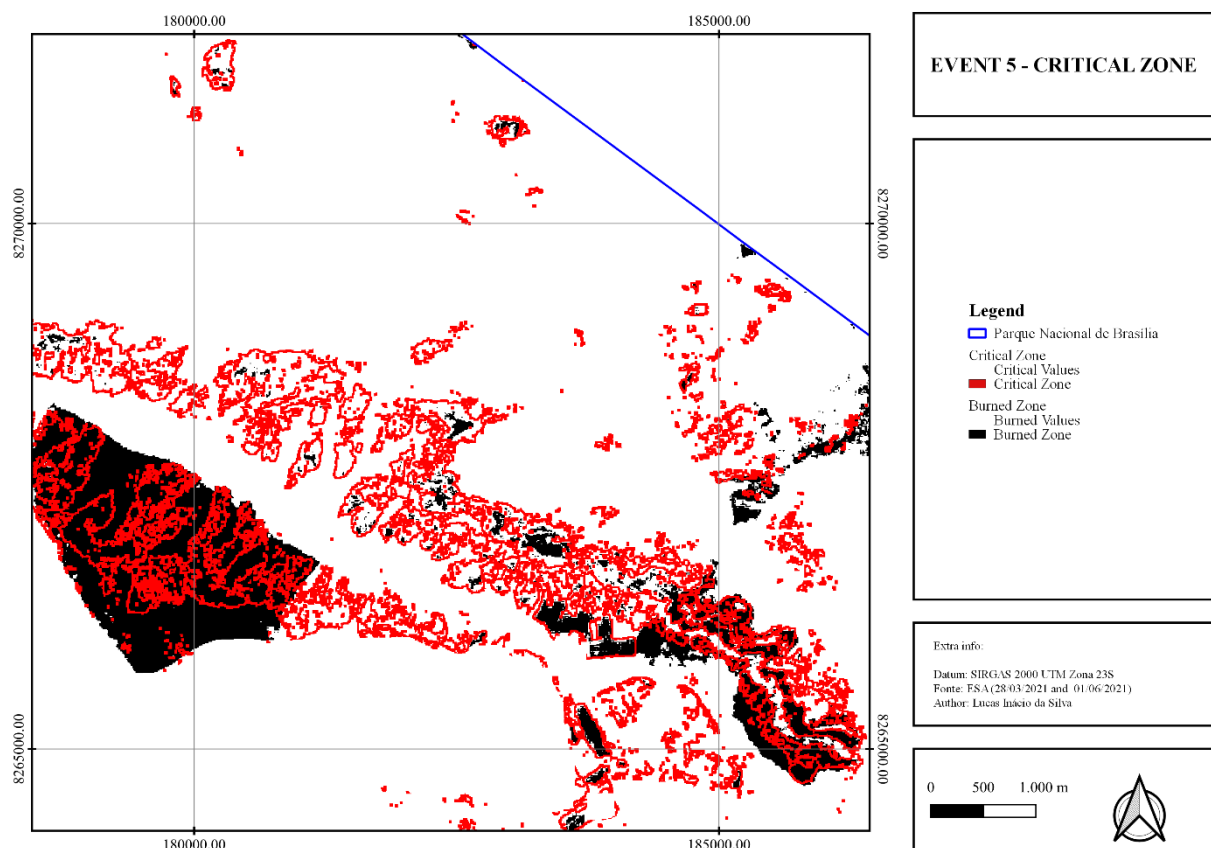
It should be noted that the climatic and vegetation context of the study region of both researches is completely different. The difference in values does not invalidate the applied methodology, since the average values found demonstrate a slightly more pessimistic perspective compared to the scenario found by Baptista et al. (2018) and Bento-Gonçalves et al. (2019).

As observed by Santos et al. (2023), the greenness values show high numbers in the rainy season. The values undergo radical changes after fire events, and indicate, before

the occurrence of the event, the susceptibility to the occurrence of fires. Although Santos et al. (2023) presents a much more refined methodology, when using machine learning techniques, the essence of the research is similar to that of the present article, since they are closely related themes and with several by-products, such as spectral indices, used in both.

Therefore, the images of the periods before the fire of the aforementioned spectral indices were manipulated, in order to isolate the values present in the critical interval found. A new image was generated, for each year, containing the superposition of each critical interval of the year with the burned pixels of the image after the fire period. Figure 10 demonstrates an example of calculating regions with fuel potential in Event 5.

Figure 10 – Critical zones in Event 5



Source: EUROPEAN SPACE AGENCE (n.d.).

It was then observed that the indication of the critical zones generated by the combination of the indexes filtered by the thresholds showed satisfactory agreement with the regions that actually burned, thus allowing the mapping of regions with fuel potential, corroborating the proposal listed by Baptista et al. (2018).

However, it should be noted that the mere spatialization of these regions can present problems such as indication of inert zones as potential fuel, indication of already burned areas as potential fuel and overestimation of critical zones.

The inert zones, such as exposed soil, are highlighted by the method due to the fact that they present a favorable spectral behavior in each index. This is due to the unfavorable valuation it receives in the indexes thanks to the type of material being observed, but it is necessary to understand that, although these areas are critical, they do not present risks of

fire propagation, such as sandbanks or gravel, for example.

The burned regions also present problems in the images, as there is an unfavorable valuation in the indices. This valuation is due to the fact that these are regions that do not present values of greenness and humidity compatible with plant structures and the values of senescence are misinterpreted, generated by the burn scar.

The years 2017, 2019, 2021 and 2022 were chosen to perform a spatial quantitative analysis using the data obtained by the thresholds, as they were the periods with the largest amounts of data extracted. Table 5 shows, in hectares, the analysis from the perspective of the area actually burned (Burned Area), the critical area obtained by the thresholds (Critical Area) and the critical area actually burned (Effective Area), obtained by the intersection of the burned area with the critical area.

**Table 5** – Quantitative analysis of critical zones

Analysis	2017	2019	2021	2022
<b>Burned Area</b>	3357.355	692.616	865.019	797.285
<b>Critical Area</b>	1742.854	19176.207	2104.648	2411.144
<b>Effective Area</b>	9.814	671.423	4.682	14.83
<b>(Effective Area) / (Burned Area)</b>	0.56%	3.50%	0.22%	0.62%
<b>(Effective Area) / (Critical Area)</b>	0.29%	96.94%	0.54%	1.86%

Source: The authors (2022).

The relationship “(Effective Area) / (Burned Area)” is observed, which indicates the percentage of the area that effectively burned, that which is within the critical region and burned at the same time, and the “(Effective Area) / (Area Critical)”, indicating how much of the critical region actually burned. The year 2019 was able to identify the critical regions well, as the burn spots were largely located within the critical regions.

## FINAL CONSIDERATIONS

It is concluded that the hypothesis previously launched was confirmed, that is, it is possible to stipulate physical thresholds that determine the range of criticality to fires by means of spectral indices. The burned regions showed a pattern of values in the indices, which explained the criticality of the region.

Greenness showed slightly more varied values, indicating that senescence and moisture are factors of greater weight in determining criticality. Moisture in the burned regions was also at the threshold of the beginning of the water stress interval. It was also observed that the average senescence of the burned region is concentrated in the region of values close to the interval that is considered the beginning of the senescence stage. The vegetation that burned had varied verdure, but had moisture and senescence favorable to fire criticality.

It is suggested to deepen the study of the determination of the critical threshold for the occurrence of fires, seeking to establish mathematical models that aim to reduce the negative effects found in the results of the spatialization of the critical regions.

It is suggested to deepen the GHG platform, with the techniques of this research, aiming to

develop a monitoring system of potential fuel regions, using free platforms and free data collection.

## REFERENCES

- BAPTISTA, G. M. M., BENTO-GONÇALVES, A., VIEIRA, A. **Avaliação das condições de verdor, umidade e de senescência da vegetação queimada no incêndio de braga, portugal, em outubro de 2017**. In: II Encontro Luso-Afro-Americano de Geografia Física e Ambiente - Desafios para Afirmar a Lusofonia na Geografia Física e Ambiente, 2018, Guimarães, Portugal. Anais (on-line). Guimarães: CEGOT-UMinho, Centro de Estudos de Geografia e Ordenamento do Território da Universidade do Minho, 2018. Available: [http://repositorium.sdum.uminho.pt/bitstream/1822/60165/1/II\\_ELAAGFA\\_Baptista\\_et\\_al.pdf](http://repositorium.sdum.uminho.pt/bitstream/1822/60165/1/II_ELAAGFA_Baptista_et_al.pdf). Access on: Apr. 29, 2023.
- BARMPOUTIS, P.; PAPAIONNOU, P.; DIMITROPOULOS, K.; GRAMMALIDIS, N. A review on early forest fire detection systems using optical remote sensing. **Sensors**, v. 20, 2020. <https://doi.org/10.3390/s20226442>
- BENTO-GONÇALVES. **Incêndios rurais – O triste fado português?** Fundação Francisco Manoel dos Santos, 2022 Available: <https://www.ffms.pt/pt-pt/atualmentes/incendios-rurais-o-triste-fado-ortugues?fbclid=IwAR2hstJhcdvec8oAhMs2vG1bZp2J2DDmoFlMorSIKrCacWCywtlj7QqrviY>. Access on: Mar. 30, 2023.
- BENTO-GONÇALVES, A.; VIEIRA, A.; BAPTISTA, G. ROCHA, J.; MOURA, SARAH. The 2017 Large wildfire of braga - evaluation of the different conditions of the burned vegetation. **Geo-Eco-Trop**, v. 43, n. 4, p. 627-640, 2019.
- CARELLA, E.; ORUSA, T.; VIANI, A.; MELONI, D.; BORGOGNO-MONDINO, E.; ORUSA, R. An integrated, tentative remote-sensing approach based on ndvi entropy to model canine distemper virus in wildlife and to prompt science-based

- management policies. **MDPI: Animals**, v. 12, n. 1049, 2022. <https://doi.org/10.3390/ani12081049>
- COLLI, G. R.; VIEIRA, C. R.; DIANESE, J. C. Biodiversity and conservation of the cerrado: recent advances and old challenges. **Biodiversity and Conservation**, v. 29, p. 1465-1475, 2020. <https://doi.org/10.1007/s10531-020-01967-x>
- DUAN, T.; CHAPMAN, S. C.; GUO, Y.; ZHENG, B. Dynamic monitoring of NDVI in wheat agronomy and breeding trials using an unmanned aerial vehicle. **Field Crop Research**, v. 210, p. 71-80, 2017. <https://doi.org/10.1016/j.fcr.2017.05.025>
- EARTH RESOURCES OBSERVATION AND SCIENCE (EROS) (USA). Washington, United States of America. Washington: EarthExplorer, 2023. 12 satellite images, color. Satellite Sentinel-2, instrument MSI. Time interval: from 05 mai 2016 to 02 mai. 2022. Lat. -15.6669, Long. -47.9997. Available on: <https://earthexplorer.usgs.gov/>. Access on: Nov. 05, 2020
- EUROPEAN SPACE AGENCY (ESA) (EUROPE). Europe: Copernicus Open Access Hub, n.d., 12 satellite images, color. Satellite Sentinel-2, instrument MSI. Time interval: from 05 mai 2016 to 02 mai. 2022. Lat. -15.6669, Long. -47.9997. Available on: <https://scihub.copernicus.eu/dhus/#/home>. Access on: Nov. 05, 2022
- FASSNACHT, F. E.; SCHMIDT-RIESE, E.; KATTENBORN, T.; HERNÁNDEZ, J. **Explaining sentinel 2-based dnbr and rdnbr variability with reference data from the bird's eye (uas) perspective**. International Journal of Applied Earth Observations and Geoinformation, n. 1, 2021. <https://doi.org/10.1016/j.jag.2020.102262>
- FERNÁNDEZ-MANSO, A.; QUINTANO, C. A synergetic approach to burned area mapping using maximum entropy modeling trained with hyperspectral data and viirs hotspots. **Remote Sensing**, v. 12, n. 858, 2020. <https://doi.org/10.3390/rs12050858>
- GEOPORTAL (Brasil). Brasília, Distrito Federal. Secretaria de Estado de Desenvolvimento Urbano e Habitação, Brasília: dados vetoriais de Cidades Administrativas, Vias Rodoviárias e Unidades de Conservação, 2022. Disponível em: <https://www.geoportal.seduh.df.gov.br/geoportal/>. Access on: Feb. 02, 2022
- GOOGLE (USA). Google Earth Engine, 2023. 12 imagens de satélite, color. Satélite Sentinel-2, instrumento MSI. Time interval: from 05 mai 2016 to 02 mai. 2022. Lat. -15.6669, Long. -47.9997. Available on: <https://code.earthengine.google.com/>. Access on: Jan. 30, 2022
- GORELICK, N.; HANCHER, M.; DIXON, M.; ILYUSHCHENKO, S.; THAU, D.; MOORE, R. GEE: planetary-scale geospatial analysis for everyone. Elsevier: **Remote Sensing Environment**, v.202, p. 18-27, 2017. <https://doi.org/10.1016/j.rse.2017.06.031>
- HARDISKY, M.A., V. KLEMAS, and R.M. SMART. The Influences of Soil Salinity, Growth Form, and Leaf Moisture on the Spectral Reflectance of *Spartina Alterniflora* Canopies. **Photogrammetric Engineering and Remote Sensing**, v. 49, p. 77-83, 1983.
- HOFMANN, G. S.; CARDOSO, M. C.; ALVES, R. J. V.; WEBER, E. J.; ALEXANDRE A. B.; TOLEDO, P. M.; PONTUAL, F. B.; SALLES, L. O.; HASENACK, H.; CORDEIRO, J. L. P.; AQUINO, F. E.; OLIVEIRA, L. F. B. The Brazilian cerrado is becoming hotter and drier. **Global Change Biology**, v. 27, p. 4060-4073, 2021. <https://doi.org/10.1111/gcb.15712>
- IBGE (Brasil). Brasília, Distrito Federal. Instituto Brasileiro de Geografia e Estatística, Brasília: dados vetoriais de biomas brasileiros. Available on: <https://www.ibge.gov.br/en/geosciences/maps/brazil-environmental-information/18341-biomes.html>. Access on: Feb. 02, 2022
- KAPLAN, G.; ADVAN, U. Object-based water body extraction model using Sentinel-2 satellite imagery. **European Journal of Remote Sensing**, v. 50, n.1, p. 137-143, 2017. <https://doi.org/10.1080/22797254.2017.1297540>
- KEY, C. H.; BENSON, N. C. **Landscape Assessment: Sampling and Analysis Methods. Landscape Assessment: Sampling and analysis Methods**, 2006.
- KEY, C. H.; BENSON, N. C. **Measuring and remote sensing of burn severity. Landscape Assessment: Sampling and analysis Methods**, 1999.
- MAGNO, R.; ROCHI, L.; DANIELLI, R.; MATESE, A.; GENNARO, S. F. D.; CHEN, C.; SON, N.; TOSCANO, P. Agroshadow: a new sentinel-2 cloud shadow detection tool for precision agriculture. **Remote Sensing**, v. 13, 2021. <https://doi.org/10.3390/rs13061219>
- MAPBIOMAS (Brazil). MAPBIOMAS: Collection Map Data – Landcover Data. Available on: <https://mapbiomas.org/download>. Access: Feb. 02, 2023.
- MARCYIN. **MarcYin/SIAC: for doi**. Belgium: Bruxelles, 2019a.
- MARCYIN. **MarcYin/SIAC\_GEE: To Publish the Code**. Belgium: Bruxelles, 2019b.
- McFEETERS, S.K. **The use of the normalized difference water index (NDWI) in the delineation of open water features**. International Journal of Remote Sensing, p. 1425-1432, 1996. <https://doi.org/10.1080/01431169608948714>
- MERZLYAK, M. N.; GITELSON, A. A.; CHIVKUNOVA, Olga B.; RAKITIN, Victor Yu. Non-destructive optical detection of pigment changes during leaf senescence and fruit ripening. **Physiologia Plantarum**, v. 106, p. 135-141, 1999. <https://doi.org/10.1034/j.1399-3054.1999.106119.x>
- MILCZAREK, M.; ROBAK, A. Sentinel Water Mask (SWM) – new index for water detection on Sentinel-2 images. **Conference: 7<sup>th</sup> Advanced Training Course on Land Remote Sensing**, 2017.
- MILLER, J. D.; THODE, A. E. Quantifying burn severity in a heterogeneous landscape with a relative version of the delta normalized burn ratio (dnbr). **Remote Sensing**, v. 109, p. 66-80, 2006. <https://doi.org/10.1016/j.rse.2006.12.006>
- NURSAPUTRA, M.; LAREKENG, S. H.; NASRI; HAMZAH, A. S. **The ndvi algorithm utilization on the GEE platform to monitor changes in forest density in mining areas**. 2nd Biennial

- Conference of Tropical Biodiversity: IOP Conf. Series: Earth and Environmental Science, 2021. <https://doi.org/10.1088/1755-1315/886/1/012100>
- RIBEIRO, N.; RUECKER, G.; GOVENDER, N.; MACANDZA, V.; PAIS, A.; MACHAVA, D.; CHAUQUE, A.; LISBOA, S. N.; BANDEIRA, R. The influence off fire frequency on the structure and botanical composition of savanna ecosystems. **Ecology and Evolution**, v. 9, p. 8253-8264, 2019. <https://doi.org/10.1002/ece3.5400>
- ROUSE, J.W.; HAAS, R.H., SCHELL, J.A.; DEERING, D.W., 1974. **Monitoring vegetation systems in the great plains with erts**. In: Proceeding Of Erts-1 Symposium. Anais ... NASA, United States.
- ROY, D. P.; BOSCHETTI, L.; TRIGG, S. N. Remote sensing of fire severity: assessing the performance of the normalized burn ratio. **Geoscience and Remote Sensing Letters**, v. 3, n. 1, 2006. <https://doi.org/10.1109/LGRS.2005.858485>
- SANTOS, S. M. B.; BENTO-GONÇALVES, A.; FRANCA-ROCHA, W.; BAPTISTA, G. **Assessment of Burned Forest Area Severity and Postfire Regrowth in Chapada Diamantina National Park (Bahia, Brazil) Using dNBR and RdNBR Spectral Indices**. *Geosciences*, v. 10, n. 106, 2020. <https://doi.org/10.3390/geosciences10030106>
- SANTOS, S. M. B.; DUBERGER, S. G.; BENTO-GONÇALVES, A.; FRANCA-ROCHA, W.; VIEIRA, A.; TEIXEIRA, G. **Remote Sensing Applications for Mapping Large Wildfires Based on Machine Learning and Time Series in Northwestern Portugal**. *Fire*, v. 6, n. 43, 2023. <https://doi.org/10.3390/fire6020043>
- SILVA, S. L.; BAPTISTA, G. M. M. Análise do grau de severidade de áreas queimadas na estação ecológica de águas emendadas por meio de dados do landsat 8. **Revista Brasileira de Geografia Física**, v. 8, n. 2, p. 431-438, 2015. <https://doi.org/10.26848/rbgf.v8.2.p431-438>
- SRIWONGSITANON, N.; GAO, H.; SAVENIJE, H. H. G.; MAEKAN, E.; SAENGSAWANG, S.; THIANPOPIRUNG, S. Comparing the normalized difference infrared index (ndii) with root zone storage in a lumped conceptual model. **Hydrology and Earth System Sciences**, v. 20, p. 3361-3377, 2016. <https://doi.org/10.5194/hess-20-3361-2016>
- SRIWONGSITANON, N.; GAO, H.; SAVENIJE, H. H. G.; MAEKAN, E.; SAENGSAWANG, S.; THIANPOPIRUNG, S. The Normalized Difference Infrared Index (NDII) as a proxy for soil moisture storage in hydrological modelling. **Hydrology and Earth System Sciences**, v. 19, 2015. <https://doi.org/10.5194/hessd-12-8419-2015>
- VERNOOIJ, R.; GIONGO, M.; BORGES, M. A.; COSTA, M. M.; BARADAS, A. C. S.; WERF, G. R. V. D. Intraseasonal variability of greenhouse gas emission factors from biomass burning in the brazilian cerrado. **Biogeosciences**, v. 1, p. 1375-1393, 2021. <https://doi.org/10.5194/bg-18-1375-2021>

## AUTHORS CONTRIBUTION

Gustavo Macedo de Mello Baptista conceived the studies with his line of research on burning metrics. Several previous studies carried out by him found strong evidence for the discretization of burned regions from unburned ones. Lucas Inácio da Silva conceived the platform for large-scale analysis of the methodology proposed by Gustavo Macedo de Mello Baptista, having also carried out the necessary validations in his area of study. The GEE platform was used under the programming knowledge of Lucas Inácio da Silva, who, under the guidance of Gustavo Macedo de Mello Baptista, created the critical threshold analysis platform.



This is an Open Access article distributed under the terms of the Creative Commons Attribution License, which permits unrestricted use, distribution, and reproduction in any medium, provided the original work is properly cited.